

# Soft Robotics for Fall Mitigation: Preliminary Design and Evaluation of a Wearable System using Continuum Robots

Param Malhotra, Nithesh Kumar, Chase Frazelle, Member, *IEEE*,  
Ian Walker, Fellow, *IEEE* and Ge Lv, Member, *IEEE*

**Abstract**— Falls can lead to serious consequences such as bone fractures or even death. Various fall protection devices such as mobile walkers, wearable airbags and lower-limb wearable robots have been developed to provide balance support or mitigate the damage from a fall. While these devices have shown promising results, critical drawbacks still exist. Most importantly, current devices can only mitigate the damage to a fall upon occurrence, but cannot take proactive action to prevent it. In this paper, we report on the design and evaluation of a novel fall prevention device using two compliant continuum robots. These two robots, which are pneumatically actuated, will be mounted to the back of a human user and deployed to grasp nearby static objects in the early stages of a fall, detected using onboard sensors. Preliminary fall experiments on a mannequin in forward, backward, and lateral directions demonstrate the efficacy of the proposed design.

## I. INTRODUCTION

Falls are common and can have a strong negative impact on people's lives. Statistics show that falls result in more than 3 million injuries being treated in emergency rooms per year in the U.S. alone, and the associated medical cost sums to \$50 billion [1]. Even for those who are not injured from a previous fall, fear of the possible consequences of future falls greatly limits their confidence, which in turn greatly limits their activities and social engagements. This can lead to further physical decline, depression and other mental issues that drastically reduce the quality of their lives [2].

Various kinds of wearable devices have been proposed to mitigate the risk of a fall. As one typical example, deployable airbags [3]–[8] are used to create a soft, flexible space between the human body and the fall environment. These devices are usually controlled in a binary “off-on” manner, simply deploying once a fall is detected and remaining inactive otherwise. The shapes of inflated airbags are inherently difficult to alter due to their intrinsic soft nature. They cannot be adjusted based on the specific direction of a fall, or to accommodate the continuously varying environment surrounding a human. Most importantly, deployable airbags can only reduce the damage to a fall afterwards, but cannot take proactive actions to prevent someone from falling down.

\*This work was supported by the South Carolina Translational Research Improving Musculoskeletal Health Faculty Development Award and U.S. National Science Foundation grants 1924721 and 2221126. The content is solely the responsibility of the authors and does not necessarily represent the official views of the NSF.

P. Malhotra and G. Lv are with the Department of Mechanical Engineering, C. Frazelle, N. Kumar, and I. Walker are with the Department of Electrical & Computer Engineering, Clemson University, Clemson, SC 29634. Corresponding Author: Ge Lv, glv@clemson.edu.

If a fall could be avoided in advance with the help of proactive devices, injuries to the human body could be possibly avoided.

Mobile walkers are also commonly used by elderly individuals to help maintain balance during walking [9], [10]. These walkers are often equipped with sensors to detect the current postures of their human users [11]–[14]. Once a possible fall is detected via real-time algorithms, some walkers can enable braking motion [11], [12] to stabilize user gaits. Alternatively, others [14], [15] aim to regulate walking speed or patterns to enhance the robustness of user gaits when navigating through different terrains. While promising, these devices typically assume that a user's gaits will be robust to external disturbances if following the walkers, but do not offer solutions for mitigating inevitable falls. Also, these walkers cannot be used for locomotion on stairs, which is an important daily task to perform that produces high fear scores among elderly individuals [16]. Even on flat terrains, a walker always goes in front of its human user during locomotion, thus is limited in or incapable of protecting humans for a backward fall induced by slips that result in more than 25% of fall associated injuries [17]. These limitations confine the use of walkers primarily for slow walking on even terrains.

Lower-limb exoskeletons are external devices that can also be controlled to help human users maintain balance. For instance, Trokov and Yi et al. investigated balance recovery strategies for bipedal locomotion and its applications to wearable robots control to help individuals recover from slip induced abnormal gaits [18]. While the results are promising, the proposed approach can only handle falls that have not yet happened or are at their early stages. If a person's Center of Mass (CoM) position deviates too much from its upright position, what can be done by the exoskeletons is limited in helping human users going back to the upright position. Asada et al. designed a lower-limb exoskeleton to act as the third leg of a person for maintaining postural balance [19], [20]. However, this device can only be used to maintain balance in a static working environment, but cannot be used for dynamic processes like falling. Existing exoskeletons simply lack safety features to mitigate the risk and damage from falls (especially for inevitable ones).

When a fall is inevitable, depending on its direction, humans tend to grasp nearby objects to maintain balance, or try to straighten their arms to minimize impact with the nearby environment when falling [21]. While this is a viable strategy in many cases, it still presents danger to the individual, as impulsive grabbing could cause arm fractures. Most importantly, humans are not able to see objects behind

their back, hence are not able to reach and grab potentially helpful objects if falling backwards. Inspired by this fact, in this paper we propose the preliminary design and evaluation of a novel fall prevention device using compliant continuum robots. Two continuum robots will be attached to the back of a human user through a customized backpack. When a possible fall has been detected by an onboard inertial measurement unit (IMU), pressure regulators will supply pressurized air so that these two robots extend or contract and bend to grasp nearby static objects for maintaining balance.

The rest of the paper is organized as follows: We begin by describing the construction of the muscles of the compliant continuum robots in Sec. II, followed by the design of the actuation system in Sec. III. We then demonstrate different fall scenarios on a mannequin and report those results in Sec. IV, followed by discussion of ongoing and future work in Sec. V.

## II. DESIGN OF COMPLIANT CONTINUUM ARMS

The robotic elements used herein to mitigate falls are rapidly deployable compliant arms. To be effective, these arms need to be able to generate sufficient force on the environment to prevent the fall, but also be sufficiently compliant to avoid the propagation of impact forces through the arms to the human. To meet these objectives we selected continuum arms [22], [23], built from pneumatically actuated artificial muscles. Continuous-bodied continuum robots are particularly suitable for this application due to their simple design, smooth profile and, particularly, their inherent compliance, which enables stable dynamic impacts with the environment [24]. Their design and implementation, along with that of a specialized gripper for rapid attachment of the arms to the environment, are described below.

### A. Design of Muscles

The core elements of the arms are pneumatic “McKibben” muscles [25]. Each individual muscle was constructed from an inner rubber tube (2.54 cm outer diameter) with high strength PET braid tightly wrapped around, fastened to the tube at the ends with metal clips. Plastic connectors at one end enabled connection to a pneumatic pressure source as the muscle input with standard tubing, and 3D-printed end caps sealed the ends of the muscles (Fig. 1). The braid was selected and connected so that increasing the input pressure to the tube caused the muscle (as constrained by the braid) to increase in length, thus creating “extensor” muscles.

### B. Design of Single Sections

Sets of three muscles were coupled together (sewn through gaps in the external braids) in parallel, to create independently controllable “sections”. Each section has three degrees of freedom: one in extension/contraction (achieved by equally increasing/decreasing pressure to the three muscles) and two in bending (achieved by differential input pressures). The length of the muscles at rest (zero pressure) was 25 cm, increasing to 35% of their unactuated length at input pressures of 65 psi. Each section was capable of bending up to 180°.



Fig. 1. Design of single muscle section. From top-left to bottom: The tubes, braids, plastic connectors, and the assembled single section arm.

### C. Design of Multi-Section Arms

The fall mitigation system features two arms, each built from a serial connection of two of the above sections. To achieve this, connector plates were 3D-printed. As shown in Fig. 2, when attached to the sections, the plates allowed the input tubes to the distal section to be routed through the muscles of the proximal section. The resulting two section arms each possess six degrees of freedom. Each arm was capable of bending up to 360° (see Fig. 3).



Fig. 2. Side-view (top left) and top-view (bottom) of the designed multi-section arm, and the end-plate (top right) that connects the two sections.

### D. Bench Top Testing

For bench top testing, we manually increased the supplied pressure to 65 psi to a single muscle, single-section arm, and multi-section arm to observe their bending angle and weight-bearing capacity, where the results are shown in Table I and Fig. 3. The single-section and multi-section arms can bend up to 180° and 360°, respectively. For the single muscle test, the muscle simply lengthens under pressure, hence the bending

angle is  $0^\circ$ . To evaluate the load bearing capacity, we hung weights on the tip of each muscle/arm until they started to deform, at maximum pressure. When fixed at one end to the back of a mannequin (described with more details in Sec. IV-A) and the other end to the environment, we demonstrated the ability of the arms to generate sufficient forces to resist falls and restore the mannequin to the upright position [26].

TABLE I  
BENCH TOP TESTING OF MUSCLES AND ARMS

Type	Max Bending	Max Load Capacity (kg)
Single Muscle	$0^\circ$	1.5
Single-Section	$180^\circ$	2.5
Multi-Section	$360^\circ$	3



Fig. 3. Maximum bending for single-section (left) and multi-section (right).

### E. Design of Passive Gripper

To enable real-time attachment of the arms to the environment, a passive adaptive gripper was designed. In contrast to active grippers, passive grippers offer the distinct advantage of requiring external power or energy only to actuate the initial grasp. No power is necessary to sustain the grip, thereby providing a built-in fail-safe in the event of power loss, making them a viable option in energy-limited or energy-scarce environments [27].

In our design, a rack and pinion system was used to close and lock the gripper when actuated by contact with the environment. Loosely inspired by the anisodactyl foot of a bald eagle where three of its four total digits are oriented forwards, and one is oriented backwards [28], the tendon driven passive gripper consists of three digits, two of which are oriented forwards and one digit oriented backwards, as shown in Fig. 4 (right).

The proximal link of the finger designed and used in the “Model O” of the Yale open hand project [29] served as the basis for the finger design. The CAD files for the base design of the fingers were obtained from the Yale open hand project. The bottom portion of the digit was modified to function as a ratchet wheel and the base part on which the digits are attached was modified to house a pawl. When assembled, the hand functions as a ratchet system that prevents the gripper from disengaging while it is actively gripping an object. The gripper consists of three main components: 1) the aforementioned digits and their bases (3 each); 2) a rack and pinion system comprised of a rack and two pinion wheels; and 3) the base of the gripper itself, which houses the other two components. The gripper measures approximately  $7.62$

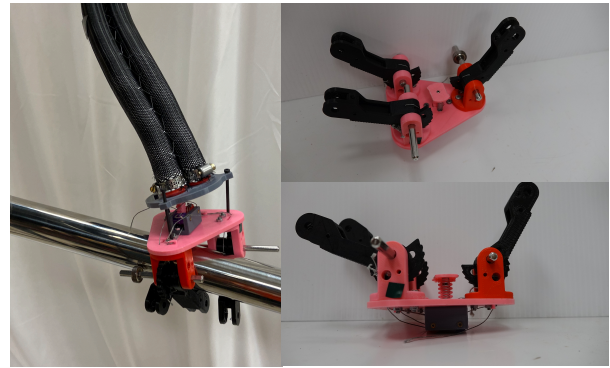


Fig. 4. Passive gripper grasping railing (left) and its two views (right).

$\times 7.62 \times 7.62$  cm, and is composed of a mix of 3D-printed parts and lightly modified off the shelf components.

The passive actuation mechanism of this tendon driven gripper is relatively straightforward. The tendon wires were anchored and wrapped around the pinion wheels, then routed through the base of the gripper and then finally through the fingers where they were terminated. The gripper engages when a downward force of sufficient magnitude is applied on the rack (hand palm) when the gripper comes in contact with an object to be grasped. This downward force on the rack causes it to displace. The displacement causes the pinion wheels to rotate, tensioning the tendon wires which in turn actuate the fingers, causing them to close and successfully grip the object of interest. The bolt pattern in the palm was matched to that on the tips of the arms, allowing easy mounting of the gripper to the arms.

### F. Integration with Backpack

The two arms were integrated with a commercially available backpack. An aluminum interior frame was constructed and installed within the backpack. As shown in Fig. 5, the two arms were mounted on this frame, emerging from the top of the backpack, at shoulder level to its wearer. The arm input tubing, muscle pressure regulators, electronics and control system hardware for the arms (to be discussed in Sec. III), were mounted on this frame, and contained within the backpack.

## III. DESIGN OF ELECTRICAL SYSTEM

In this section, we present the selection of necessary sensors, actuation units, and control components to detect a fall online and take corresponding control actions.

### A. Actuation Selection

We chose twelve electro-pneumatic pressure regulators (ITV1050-31N1N4, SMC Corporation, Fig. 6, right) to control the input air pressure to each of the six muscles for the two sections of each arm. A single input line from an air compressor simultaneously connected all regulators’ inputs. The power/data cables were connected to each regulator, and the internal feedback control system of the regulator ensures the desired pressure output to all muscles.



Fig. 5. Designed backpack with two arms attached. The electronics and pressure regulators will be introduced in Sec. III and Fig. 6.

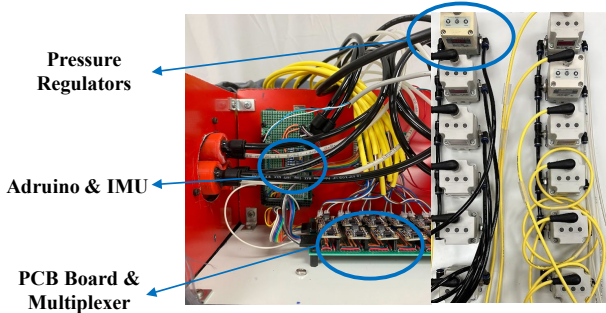


Fig. 6. Electrical components (left) and pressure regulators (right) inside the designed backpack.

### B. Sensors & Actuators

To detect falling, we used an IMU sensor (MPU-6050, InvenSense, CA) to measure the tilting angle of the backpack from the upright position. This angular information has been widely used as an indicator to determine if a person falls down [30]. Under the assumption that the z-axis of the IMU is perpendicular to the sagittal plane, we converted this rotation matrix to a global sagittal-plane angle for a human torso. The IMU is placed on the board that separates the lower and upper part of the backpack (Fig. 6, left) in order to align with the sagittal plane. A suite of DACs (MCP 47250) converted control signals to analog inputs for each regulator. The outputs of the regulators (an analog signal reporting the actual pressure output of each) were handled through a multiplexer placed on a custom PCB board. All the above sensory feedback were sent to an Arduino Mega 2560 Rev3 for calculating control commands. The entire electrical system is powered by a power supply unit (LRS-150, 24V/6.5A, MEAN WELL, Taiwan).

### C. Control Architecture

In the experiments reported herein, we used a simple Proportional-Derivative (PD) controller to regulate the pressure supplied to the robots, i.e.,

$$u = -K_p(\theta - \bar{\theta}) - K_d(\dot{\theta} - \dot{\bar{\theta}}), \quad (1)$$

where  $u$  is the control command,  $\theta$  and  $\dot{\theta}$  are the sensed angular position and velocity of the backpack, and  $\bar{\theta}$  and  $\dot{\bar{\theta}}$  are the equilibrium position and velocity. The PD gains  $K_p$  and  $K_d$  were tuned through trial and error, which will be specified in Sec. IV-A. The simplicity of the control method allowed for all computation and I/O handling to take place on the Arduino, without the need for external resources.

## IV. PRELIMINARY EXPERIMENTAL EVALUATIONS

Having completed the design, we performed preliminary testing to verify the efficacy of the continuum arms. We first mounted the backpack to a mannequin to conduct experiments in backward, forward, and lateral directions, and then conducted tests with the passive gripper.

### A. Fall Experiments with a Mannequin

The mannequin selected for the fall experiments did not have flexible limbs, and was designed to be balanced on a stand (white plate in Fig. 7) instead of its feet. This feature prevented the mannequin from falling freely without slipping, as the mannequin did not have rotating ankle joints. Therefore, in order to simulate falling, we used the extensibility of the continuum arms to lower the mannequin to a fallen state, and then used the controller to return the mannequin to equilibrium or upright position. For fall experiments, the mannequin was placed between two parallel bars, which provided fixed environmental features within the reachable range of the arms for the system to attach to during the experiments.

We conducted a series of forwards, backwards, and lateral fall experiments, where screenshots of the backward falling is shown in Fig. 7. The video accompanying this paper shows examples of all cases. The key goal of these tests was to evaluate the capability of the arms, when connected to the environment, to constrain the mannequin from falling and to restore it to the vertical position. Therefore, for these tests, the tips of the arms were fixed to the rails. Active grasping of the rails with the gripper will be discussed in the following subsection.

### B. Gripper Testing

To determine the limits for the gripper, we incrementally increased a mass hanging from the gripper while connected to a digital hanging scale. The gripper was able to handle a mass of 26.29 kg. The versatility of the gripper was tested by grasping various objects such as railings, table edges, and cylinders of various diameters (maximum of 5.1 cm). When mounted on the continuum arms, the gripper was swung towards the railings around the mannequin and was shown to be able to successfully grasp the railing (Fig. 4, left) and maintain a stable grasp.

### C. Results & Discussion

For all fall tests, we first calibrated the IMU sensors when the mannequin was at its upright position to record this position as  $\bar{\theta}$  (initial). Due to the way that the arms were attached, the initial upright position was slightly different.

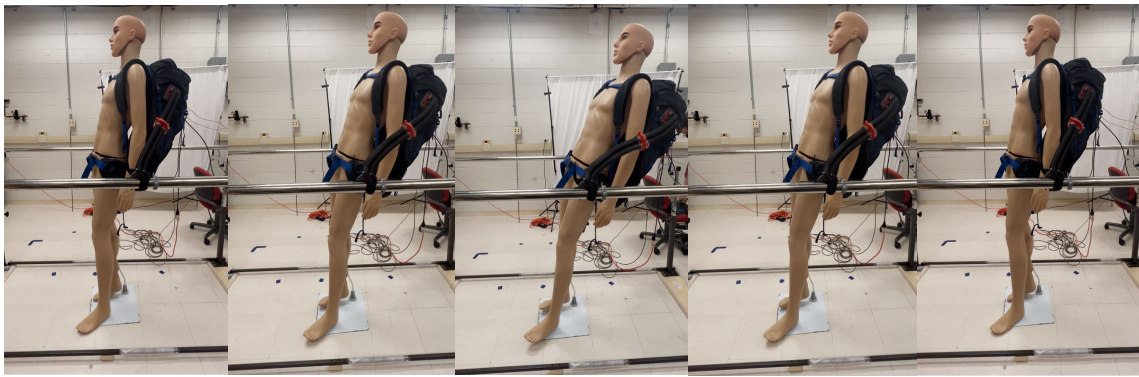


Fig. 7. Screenshots of the mannequin falling backwards while the arms were deployed to restore the upright position.

The desired position  $\bar{\theta}$  (mid) was then set to a value to enable extension motion of the arms to pull the mannequin away from its upright position. Once the mannequin reached the fallen state, we manually changed the desired position  $\bar{\theta}$  back to zero to enable contraction motion for the arms. The desired positions as well as the PD gains are summarized in Table II, and the experimental results are demonstrated in Fig. 8. For consistency, we denoted all desired positions  $\bar{\theta}$  to be negative once the mannequin was tilted, and we kept  $K_p$  and  $K_d$  consistent for each fall case.

From Fig. 8, we can see that the arms reacted appropriately (within 2 seconds) to pull the mannequin back to its upright position. The corresponding pressure values demonstrated that the pressure regulators acted rapidly once the difference between the current and desired positions were detected. Note that the regulator's pressure was saturated at 55 psi to ensure safety. When this saturation was released, we could further reduce the reaction time for the experiments.

TABLE II  
PARAMETERS FOR PD CONTROLLER

Case	$\bar{\theta}$ (initial)	$\bar{\theta}$ (mid)	$K_p$	$K_d$
Backward	0°	-13°	45	0.7
Forward	-1°	-9°	30	0.7
Sideways	0°	-16°	40	0.7

## V. LIMITATIONS & FUTURE WORK

The preliminary experimental results presented in this paper served as a proof of concept study for the overall design and control, therefore limitations exist in both the design and control aspects. Firstly, this paper adopts a simple PD controller to regulate the supplied pressure to the arms, which is only dependent on the mannequin's tilting angle and its velocity. This simple controller did not take the complex nature of human behaviors during a fall into account, therefore is limited in performance. Moreover, we assumed all falls occurred perfectly in one plane, which is generally not true for human falls. In the future, we will utilize angular information from all three axes of the IMU sensor and better determine the fall direction. Meanwhile, we will develop model-based controllers for the arms to allow them to quickly deploy to grasp environmental objects sensed in real time.

Secondly, all fall experiments were conducted on a mannequin that was not able to fall freely due to its mechanical structure. The testing reported herein is restricted to cases with the backpack attached to a mannequin. As discussed in Sec. IV-A, we will need to manually initiate the fall process by first extending the arm. In the future, we will attach the designed backpack to a more human-like mannequin with flexible joints to allow free falls, and transition to testing with human subjects.

Finally, the general trajectories of the arms were pre-selected to propel them towards the rails, with the compliance of the arms and adaptive triggering of the gripper used to successfully complete the grasps. The locations of the fixed environmental features used for support, i.e., the railings, with respect to the backpack were known a priori. Future work will include active sensing of the rails, and of more general environmental objects.

## REFERENCES

- [1] "Get the Fact on Falls Prevention, National Council on Aging," <https://www.ncoa.org/article/get-the-facts-on-falls-prevention>, accessed: 2021-10-21.
- [2] B. J. Vellas, S. J. Wayne, L. J. Romero, R. N. Baumgartner, and P. J. Garry, "Fear of falling and restriction of mobility in elderly fallers," *Age and ageing*, vol. 26, no. 3, pp. 189–193, 1997.
- [3] G. Shi, C.-S. Chan, Y. Luo, G. Zhang, W. J. Li, P. H. Leong, and K.-S. Leung, "Development of a human airbag system for fall protection using mems motion sensing technology," in *2006 IEEE/RSJ International Conference on Intelligent Robots and Systems*. IEEE, 2006, pp. 4405–4410.
- [4] T. Tamura, T. Yoshimura, M. Sekine, M. Uchida, and O. Tanaka, "A wearable airbag to prevent fall injuries," *IEEE Transactions on Information Technology in Biomedicine*, vol. 13, no. 6, pp. 910–914, 2009.
- [5] Z. Zhong, F. Chen, Q. Zhai, Z. Fu, J. P. Ferreira, Y. Liu, J. Yi, and T. Liu, "A real-time pre-impact fall detection and protection system," in *2018 IEEE/ASME International Conference on Advanced Intelligent Mechatronics (AIM)*. IEEE, 2018, pp. 1039–1044.
- [6] G. Wu and S. Xue, "Portable preimpact fall detector with inertial sensors," *IEEE Transactions on neural systems and Rehabilitation Engineering*, vol. 16, no. 2, pp. 178–183, 2008.
- [7] K. Fukaya and M. Uchida, "Protection against impact with the ground using wearable airbags," *Industrial health*, vol. 46, no. 1, pp. 59–65, 2008.
- [8] S. Ahn, D. Choi, J. Kim, S. Kim, Y. Jeong, M. Jo, and Y. Kim, "Optimization of a pre-impact fall detection algorithm and development of hip protection airbag system," *Sensors and Materials*, vol. 30, no. 8, pp. 1743–1752, 2018.

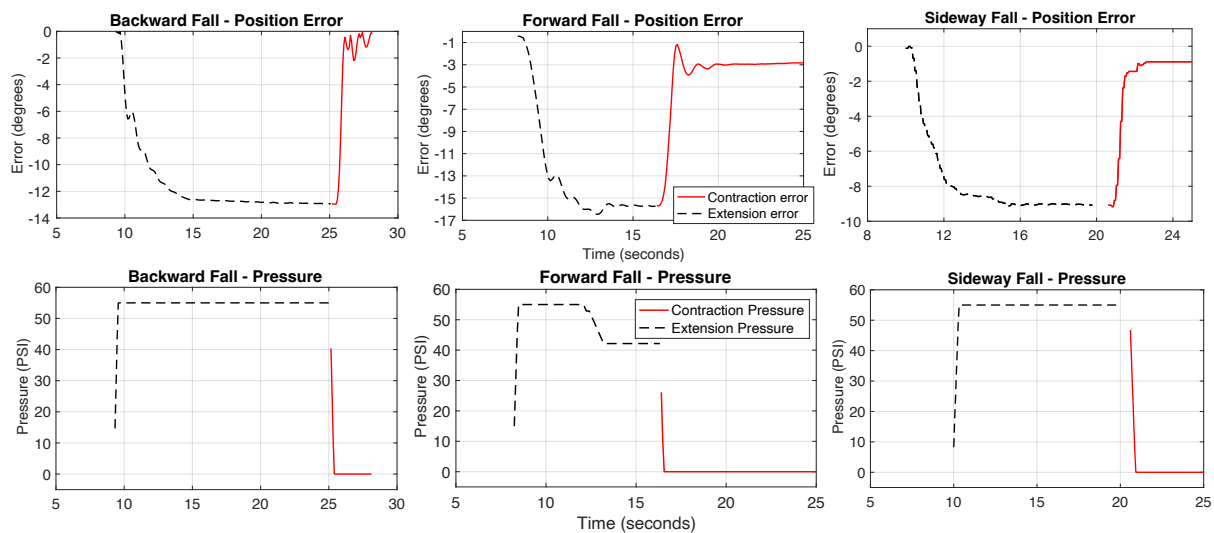


Fig. 8. Errors between the mannequin's current sagittal plane position and the desired position (top row) and pressure values from the regulators (bottom row) for backward (left), forward (center), and sideways falls (right). The  $x$ -axes for all figures are duration of the experiments, and the center figure legends apply to all figures.

- [9] M. Martins, C. Santos, A. Frizera, and R. Ceres, "A review of the functionalities of smart walkers," *Medical engineering & physics*, vol. 37, no. 10, pp. 917–928, 2015.
- [10] M. M. Martins, C. P. Santos, A. Frizera-Neto, and R. Ceres, "Assistive mobility devices focusing on smart walkers: Classification and review," *Robotics and Autonomous Systems*, vol. 60, no. 4, pp. 548–562, 2012.
- [11] Y. Hirata, S. Komatsuda, and K. Kosuge, "Fall prevention control of passive intelligent walker based on human model," in *International Conference on Intelligent Robots and Systems*. IEEE/RSJ, 2008, pp. 1222–1228.
- [12] K. Hirota and T. Murakami, "Imu sensor based human motion detection and its application to braking control of electric wheeled walker for fall-prevention," *IEEJ Journal of Industry Applications*, vol. 5, no. 4, pp. 347–354, 2016.
- [13] A. R. da Silva and F. Sup, "Design and control of a two-wheeled robotic walker for balance enhancement," in *International Conference on Rehabilitation Robotics (ICORR)*. IEEE, 2013, pp. 1–6.
- [14] A. R. da Silva and F. C. Sup, "A robotic walker based on a two-wheeled inverted pendulum," *Journal of Intelligent & Robotic Systems*, vol. 86, no. 1, pp. 17–34, 2017.
- [15] J. Glover, D. Holstius, M. Manojlovich, K. Montgomery, A. Powers, J. Wu, S. Kiesler, J. Matthews, and S. Thrun, "A robotically-augmented walker for older adults," *Technical Report CMU-CS-03-170*, 2003.
- [16] M. E. Lachman, J. Howland, S. Tennstedt, A. Jette, S. Assmann, and E. W. Peterson, "Fear of falling and activity restriction: the survey of activities and fear of falling in the elderly (safe)," *The Journals of Gerontology Series B: Psychological Sciences and Social Sciences*, vol. 53, no. 1, pp. P43–P50, 1998.
- [17] T. E. Lockhart, J. L. Smith, and J. C. Woldstad, "Effects of aging on the biomechanics of slips and falls," *Human factors*, vol. 47, no. 4, pp. 708–729, 2005.
- [18] M. Mihalec, M. Trkov, and J. Yi, "Balance recoverability and control of bipedal walkers with foot slip," *Journal of biomechanical engineering*, 2021.
- [19] D. J. Gonzalez and H. H. Asada, "Hybrid open-loop closed-loop control of coupled human-robot balance during assisted stance transition with extra robotic legs," *IEEE Robotics and Automation Letters*, vol. 4, no. 2, pp. 1676–1683, 2019.
- [20] D. J. Gonzalez and H. H. Asada, "Passive quadrupedal gait synchronization for extra robotic legs using a dynamically coupled double rimless wheel model," in *2020 IEEE International Conference on Robotics and Automation (ICRA)*. IEEE, 2020, pp. 3451–3457.
- [21] B. E. Maki and W. E. McIlroy, "Control of rapid limb movements for balance recovery: age-related changes and implications for fall prevention," *Age and ageing*, vol. 35, no. suppl.2, pp. ii12–ii18, 2006.
- [22] I. D. Walker, "Continuous backbone: "Continuum" robot manipulators," *ISRN Robotics*, vol. 2013, pp. 1–19, 2013.
- [23] M. E. Stokes, J. K. Mohrmann, C. G. Frazelle, I. D. Walker, and G. Lv, "The claw: An avian-inspired, large scale, hybrid rigid-continuum gripper," *Robotics*, vol. 13, no. 3, p. 52, 2024.
- [24] M. Wooten and I. Walker, "Environmental interaction with continuum robots exploiting impact," *IEEE Robotics and Automation Letters*, vol. 7, no. 4, pp. 10136–10143, 2022.
- [25] B. Tondu, "Modelling of the mckibben artificial muscle: A review," *Journal of Intelligent Materials and Structures*, vol. 23, no. 3, pp. 225–253, 2012.
- [26] P. Malhotra, *Soft Robotic Arms for Fall Mitigation: Design, Control, and Evaluation*. Clemson University: M.S. Thesis, Department of Mechanical Engineering, 2022.
- [27] W. Crooks, S. Rozen-Levy, B. Trimmer, C. Rogers, and W. Messner, "Passive gripper inspired by manduca sexta and the fin ray effect," *International Journal of Advanced Robotic Systems*, vol. 14, no. 4, 2017.
- [28] J. F. Botelho, D. Smith-Paredes, D. Nuñez-Leon, S. Soto-Acuna, and A. O. Vargas, "The developmental origin of zygodactyl feet and its possible loss in the evolution of passeriformes," *Proceedings of the Royal Society B: Biological Sciences*, vol. 281, no. 1788, p. 20140765, 2014.
- [29] R. Ma and A. Dollar, "Yale openhand project: Optimizing open-source hand designs for ease of fabrication and adoption," *IEEE Robotics & Automation Magazine*, vol. 24, no. 1, pp. 32–40, 2017.
- [30] Y. Yan and Y. Ou, "Accurate fall detection by nine-axis imu sensor," in *2017 IEEE International Conference on Robotics and Biomimetics (ROBIO)*. IEEE, 2017, pp. 854–859.